GEM TN-93-376

Pileup Noise in GEM Liquid Ionization Calorimeter

W.E. Cleland
University of Pittsburgh

A.V. Vanyashin
SSC Laboratory

June 17, 1993

Abstract:

Results of a pileup noise study in GEM liquid krypton and liquid argon calorimeters are presented. The GEM liquid ionization calorimeters are designed in the way that pileup noise do not dominate in electromagnetic resolution.

Pileup Noise in GEM Liquid Ionization Calorimeter

W.E. Cleland
University of Pittsburgh
Pittsburgh, PA 15260

A.V. Vanyashin *
SSC Laboratory
Dallas, TX 75237

June 17, 1993

Abstract

Results of a pileup noise study in GEM liquid krypton and liquid argon calorimeters are presented. The GEM liquid ionization calorimeters are designed in the way that pileup noise do not dominate in electromagnetic resolution.

1 Introduction

SSC physics goals (*e.g.*, Higgs search via the $H^0 \to \gamma\gamma$ decay) require detectors with high electromagnetic resolution. To achieve this goal the different sources of the noise in the detector should be well understood.

At the SSC with a luminosity of $10^{33}\text{cm}^{-2}\text{s}^{-1}$ an average of 1.6 (non-diffractive) minimum bias events occur during every bunch crossing. The same (on average) number of minimum bias events also occur during the bunch crossing in which the rare event of interest happens. Because at the SSC the interval between the events (16.7 ns) is shorter than a data collection time for an event, not only the minimum bias events from the bunch crossing that is on-time with the event of interest contribute to the measured signal, but also events from other (out-of-time) bunch crossings. As particles from those pileup events typically deposit low energies in the calorimeter ($E_T \lesssim 0.5$ GeV), for the calorimeter signal of interest ($E_T \gtrsim 16$ GeV) their effect can be considered as a noise. We denote by ρ_p^2 the variance of the transverse energy deposited per unit time in a calorimeter cell. The variance in the detected signal due to this type of noise is an incoherent sum of contributions from the previous crossings:

$$\sigma_p^2 = \rho_p^2 T_c \sum w_i^2 = \rho_p^2 S_p.$$

The summation is over the normalized signal waveform w_i, evaluated at the time points spaced by the beam crossing interval of $T_c = 16.7$ ns. Thus the pileup noise is made up of two factors, the pileup noise density coming from the fluctuations in the energy deposition

*Permanent address: Moscow Engineering Physics Institute, Moscow, Russia

arising from high cross section interactions, and the pileup sum S_p, coming from the choice of shaping function. For $(CR)^2(RC)^6$ filtering with peaking times in the range of 50–100 ns, the approximate value of S_p is

$$S_p \sim 2t_p,$$

where t_p is the peaking time.

It is important to account for the effects of pileup noise in the calorimeter design. In particular the size of the electromagnetic calorimeter cells and the peaking time of the read-out electronics should be chosen so that the pileup noise will not be dominant in the calorimeter resolution for energies of the processes of interest to GEM. In this note we demonstrate that the expected value of the pileup noise in the GEM calorimeter satisfies the above criteria. Section 2 describes the model used to simulate the effect of the pileup noise in the GEM calorimeters. The results of the simulation are presented in Section 3. Due to the low pileup occupancy in the GEM calorimeters (for small areas) the pileup noise distribution is non-Gaussian. It is important to account for this feature in trigger studies and in studies of jet rejection by isolation. As can be seen from Fig. 1, the approach we use to simulate the effect of the pileup noise gives a larger and more realistic fluctuations and a smaller typical value than the equivalent Gaussian noise (with the same R.M.S.). The non-Gaussian tail of the pileup noise affects the signal efficiency for, *e.g.*, the γ/jet rejection by isolation. Section 4 describes the effect of the pileup noise on jet rejection by isolation.

2 Model for pileup noise

To determine the effects of out-of-time pileup, a Poisson-distributed number of minimum bias events is generated for each 56 preceding and 13 following bunch crossings. To study the response of the GEM forward calorimeter, the 2.0 (on average) minimum bias events were generated for every bunch crossing with PYTHIA 5.6, including the single- and double-diffractive events.

The GEM calorimeter response to the generated events was simulated with `gemfast`. Since we are interested in the pileup effects in the electromagnetic and hadronic parts of calorimeter separately, it is important simulate properly the fluctuations in the shower development. The parameterized response of the calorimeter implemented in `gemfast` includes shower profiles and energy resolution. Longitudinal and transverse electromagnetic and hadronic shower profiles are generated using GFLASH 1.3 [1], which was originally developed to describe the H1 liquid argon calorimeter. GFLASH incorporates correlated fluctuations of shower profile parameters, hadronic shower fluctuations into early π^0's, transverse profile changes with depth, and shower development along the true direction of incidence as determined by tracking through the central tracker region. It gives a good description of the shapes of both electromagnetic and hadronic showers in uniform regions of the calorimeter. In Fig. 2 we show, for example, the fraction of hadronic showers which is electromagnetic in nature. This distribution matches well the one produced by detailed shower simulation, but it is not reproduced by the Bock parameterization that has been used in previous pileup studies [2].

The GEM calorimeter in `gemfast` is segmented longitudinally in only three sections – the EM calorimeter, the liquid hadronic calorimeter and the scintillating barrel calorimeter. The further longitudinal division of GEM EM and hadronic calorimeters was not taken into account. In particular, the pileup noise in the EM calorimeter strips is not addressed by this study. Another approximation in this study was the segmentation of the endcap calorimeter in $\eta \times \phi$, which is different from GEM TDR design. Figure 3 shows the GEM calorimeter segmentation, as implemented in `gemfast`.

The calorimeter response for each bunch crossing is weighted with the response function w_i, and the sum for each cell is calculated to provide a snapshot of the response of the calorimeter to pileup. This insures that all the longitudinal and transverse correlations among cells are preserved. Figure 4 shows the normalized signal waveform, w_i, for different parts of the GEM calorimeter. The parameters of the $(CR)^2(RC)^6$ shaping circuit were adjusted in a way to provide a measurement time of 40 ns for the EM part of the calorimeter and 100 ns for the hadronic part.

For the studies of the physics performance of the GEM detector one of these snapshots is then superimposed on the response from the signal and in-time pileup events. This approximation represents the case of just one sampling and thus is a conservative estimate of the pileup effects. GEM TDR baseline design assumes that 5 samples of the calorimeter signal would be used for the subsequent optimal filtering (or possibly in the off-line) analysis. Such an analysis can reduce the total noise (thermal + pileup) by 20% if the hardware shaping time is optimally chosen. This reduction is considerably more if the shaping time is not near the optimal value. This would be the case for the initial SSC running, with the luminosity below $10^{33}\mathrm{cm}^{-2}\mathrm{s}^{-1}$.

3 Pileup noise in the GEM calorimeter

The generated calorimeter snapshots were used to determine the expected pileup noise distributions in the GEM calorimeter. Figure 5 shows the pileup noise distribution for the large cones relevant for a measurement of jet energy and for jet rejection by isolation. The distributions are Gaussian due to a high pileup occupancy for large calorimeter areas.

For processes that require precision energy measurements the pileup noise in a small area of the EM calorimeter is relevant. Figure 6 shows the pileup distributions for small areas of the endcap calorimeter (with no thermal noise added). The difference in the R.M.S. of the pileup noise and the sigma of the Gaussian fit to the distribution is a result of a low pileup occupancy in the GEM calorimeter for small areas.

For the physics processes of interest at the SSC the relevant measure of the pileup noise in small areas is the width parameter from a Gaussian fit to the pileup distribution. The width of the Higgs mass resolution measured via $H^0 \to \gamma\gamma$ decay calculated using gemfast with pileup from the generated calorimeter snapshots agree with the Higgs width estimated from the simple parameterization of the pileup noise using the width from the fit values [3]. In this note we used the fitted widths to characterize the pileup noise.

Figure 7 shows the pseudorapidity dependence of the pileup noise. Note that there is no significant difference in pileup noise for LKr and LAr EM calorimeters. This is because despite the factor of 1.5 difference in a drift time for the LKr and LAr the difference in the pileup sum S_p is small. For the EM calorimeter $S_p^{\mathrm{LKr}} = 70$ ns and $S_p^{\mathrm{LAr}} = 72$ ns. For the hadronic calorimeter $S_p^{\mathrm{LKr}} = 184$ ns and $S_p^{\mathrm{LAr}} = 190$ ns.

The rapidity dependence for, *e.g.*, the 5×5 tower sum on Figure 7 is entirely due to an increase with rapidity of the EM tower size in $\Delta\eta \times \Delta\phi$ (see Figure 3). Figure 8 shows the pseudorapidity dependence of the pileup noise for the small cones of fixed area in $\Delta\eta \times \Delta\phi$. In agreement with previous study of pileup noise [2], no significant rapidity dependence is observed (for fixed calorimeter area).

To account for the difference in the sigma from the fit and the R.M.S. of the pileup distribution at small area values one can estimate the pileup noise density as:

$$\rho_p = \sigma_p / \sqrt{S_p}.$$

Here σ_p is the width parameter from a Gaussian fit to the pileup noise distributions for

different calorimeter areas. This definition is somewhat different from the one in [2], in which ρ_p^2 is the variance of the distribution. Figure 9 shows the pileup noise density for the EM and hadronic LAr calorimeter sections for different areas centered at $\eta = 0.117$. Note that the pileup noise density is about four times less in the hadronic section than in the EM section. The solid line on the plot represents the fit to the area dependence for the EM part:

$$\rho_p^{\mathrm{EM}} = 0.46\mathrm{GeV}/\sqrt{\mathrm{ns}}A^{0.89}.$$

Here A is the calorimeter area in $\Delta\eta \times \Delta\phi$. Pileup noise is growing faster than $\sqrt{A}$ due to multiparticle correlations arising from jets and from correlations in time due to the Poisson distribution of events in each crossing.

Figure 10 shows the pileup noise density for the sum of both EM and hadronic sections. As the pileup noise in EM section is dominant, we used the S_p value of EM calorimeter (70 ns). The solid line on the plot is a fit to the data: $\rho_p = 0.66$ GeV$/\sqrt{\mathrm{ns}}A^{0.94}$. The pileup noise density values agree with the ones estimated from the phenomenological parameterization from [2]: ρ_p =0.38 GeV$/\sqrt{\mathrm{ns}}A^{0.76}$, (shown by the dotted line on the plot). The relatively small difference from the previous results [2] can be attributed to the use of a different event generator (ISAJET) and shower parameterization algorithm (QFL).

4 Jet rejection by isolation

The physics signatures of interest at the SSC involve identification of isolated photons and electrons. Since the cross-section of the processes of interest is small and the potential backgrounds are large, this identification requires a rejection factor of $10^{-3} - 10^{-4}$ for QCD jets. A crucial role in jet rejection for γ and e identification in GEM is played by a calorimeter isolation cut that can be done requiring

$$\sum E_T - E_T^{\gamma/e} < E_T^{\mathrm{mean}} + E_T^{\mathrm{cut}}.$$

Here the sum is over calorimeter tower with centers inside a cone of radius R. The transverse energy of the γ/e candidate, $E_T^{\gamma/e}$, is subtracted from the sum. E_T^{mean} is the mean transverse energy in the cone, due to a pileup and thermal noise; and E_T^{cut} is the isolation threshold imposed.

Figure 11a shows the total noise in a cone of radius $R = 0.45$ centered at $\eta = 0.117$. Table 1 presents the efficiency loss for different values of E_T^{cut}. The non-Gaussian tail in the noise distribution makes the efficiency loss for a typical isolation cut of 3–5 GeV unacceptably high. To reduce the noise effect on efficiency one can include in the sum only the calorimeter cells with $|E_T| > 0.5$ GeV. This reduces the width (from the Gaussian fit) of the noise distribution from 3.4 GeV to 1.7 GeV, as shown in Figure 11. Table 1 shows that summing only the cells with $|E_T| > 0.5$ GeV in the isolation sum reduces the efficiency loss due to a noise by a factor of about two. Another approach, not evaluated here but essentially equivalent to the above, would be to demand that each cell within the cone be below a threshold which could substantially lower than the values used above, due to the lower thermal and pileup noise in an individual cell.

5 Conclusions

We have studied the pileup noise in the GEM liquid ionization calorimeters with gemfast simulation package. PYTHIA was used to generate minimum bias events and GFLASH was used to simulate the calorimeter response. The expected values of pileup noise agree with

Table 1: Efficiency loss due to an isolation cut on $E_T^{cut} + E_T^{mean}$ in a $R = 0.45$ cone.

Cells included in the sum	E_T^{mean} (GeV)	E_T^{cut} (GeV)	Efficiency loss (%)
All cells	0.22	5	10.2± 0.6
		4	13.3
		3	18.9
Cells with $\|E_T\|$ >0.5 GeV	1.48	5	5.4 ± 0.4
		4	7.6
		3	11.0

the previous estimates [2], that were obtained using a different event generator (ISAJET) and parameterized calorimeter response (QFL).

Figure 12 shows the GEM EM calorimeter resolution (corresponding to the GEM TDR design) with the contribution of different factors. Figure 12 demonstrates that the expected value of the pileup noise in the GEM EM calorimeter does not dominate in electromagnetic resolution, due to a proper choice of the electromagnetic calorimeter cells size and the measurement time of the read-out electronics.

6 Acknowledgments

We would like to thank Hong Ma, Ken McFarlane, Tomasz Skwarnicki, and all our other GEM colleagues whose work on simulations made this study possible.

References

[1] G. Grindhammer et al., Proc. of the Workshop on Calorimetry for the Supercollider, Tuscaloosa, AL, 1989, p.151, SLAC-PUB-5072, 1989 and Nucl. Inst. and Meth. **A290**, 469 (1990).

[2] W.E. Cleland and E.G. Stern, Signal Processing for Liquid Ionization Calorimeters, in Proc. of III Int. Conference on Calorimetry, Corpus Christi, Sep 29–Oct 2, 1992.

[3] Hong Ma, private communication.

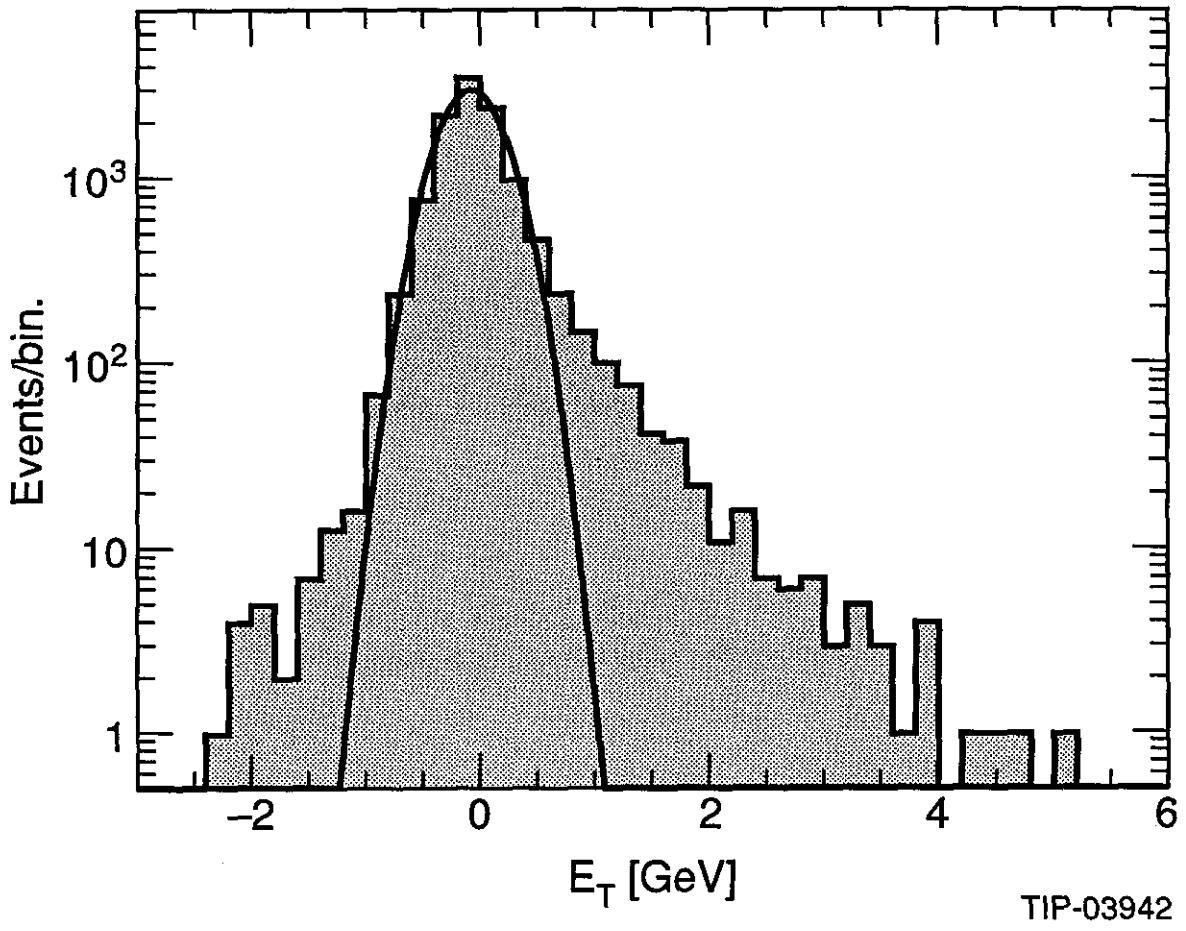

Figure 1: Histogram of the distribution of the signal after shaping, caused by pileup (both in-time and out-of-time) events for a 0.16×0.16 electromagnetic trigger tower. The curve shows a Gaussian fit, which obviously does not describe the data well.

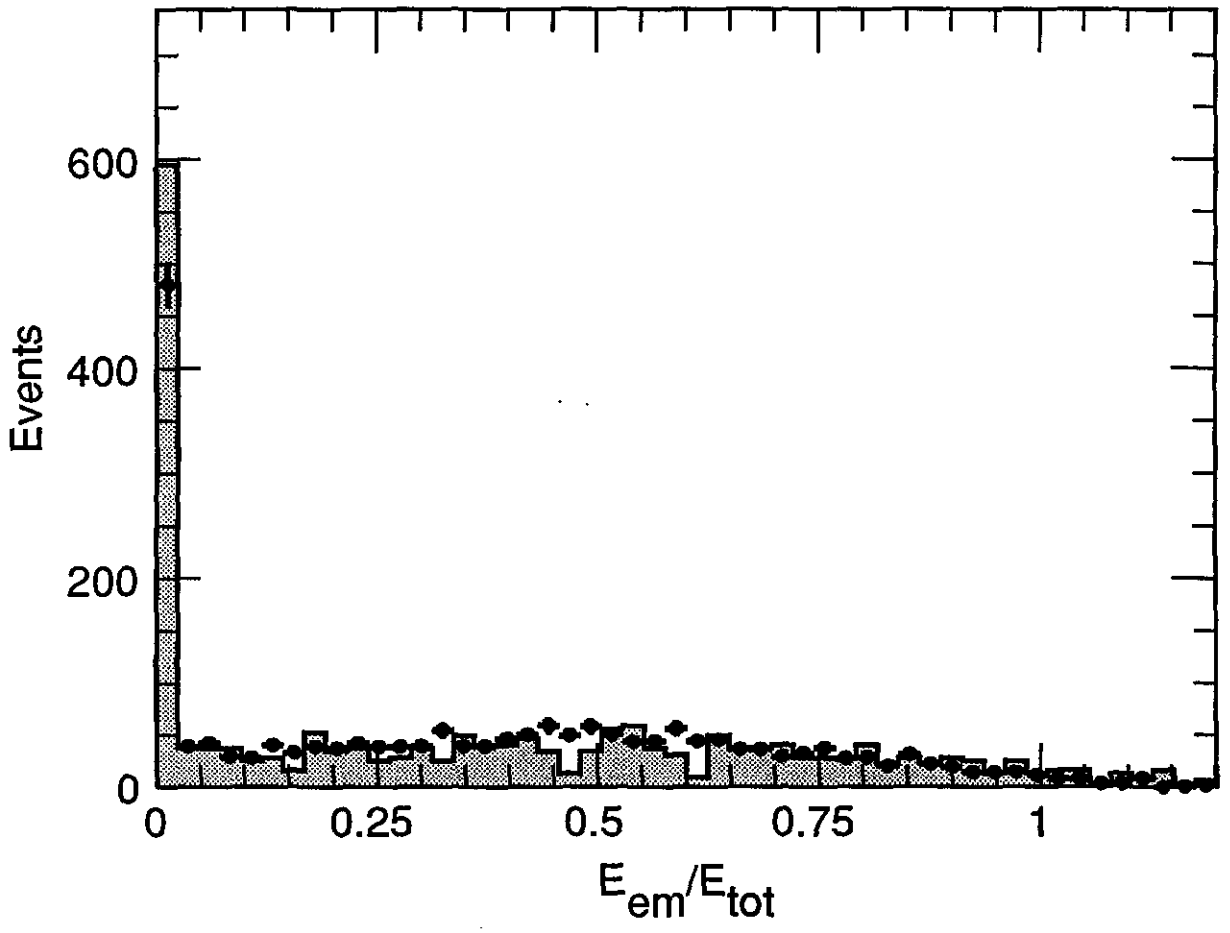

Figure 2: Ratio of electromagnetic to total energy for 100 GeV π's. The histogram shows the result of a full GEANT simulation, and the points show the GFLASH-based parameterization used in `gemfast`.

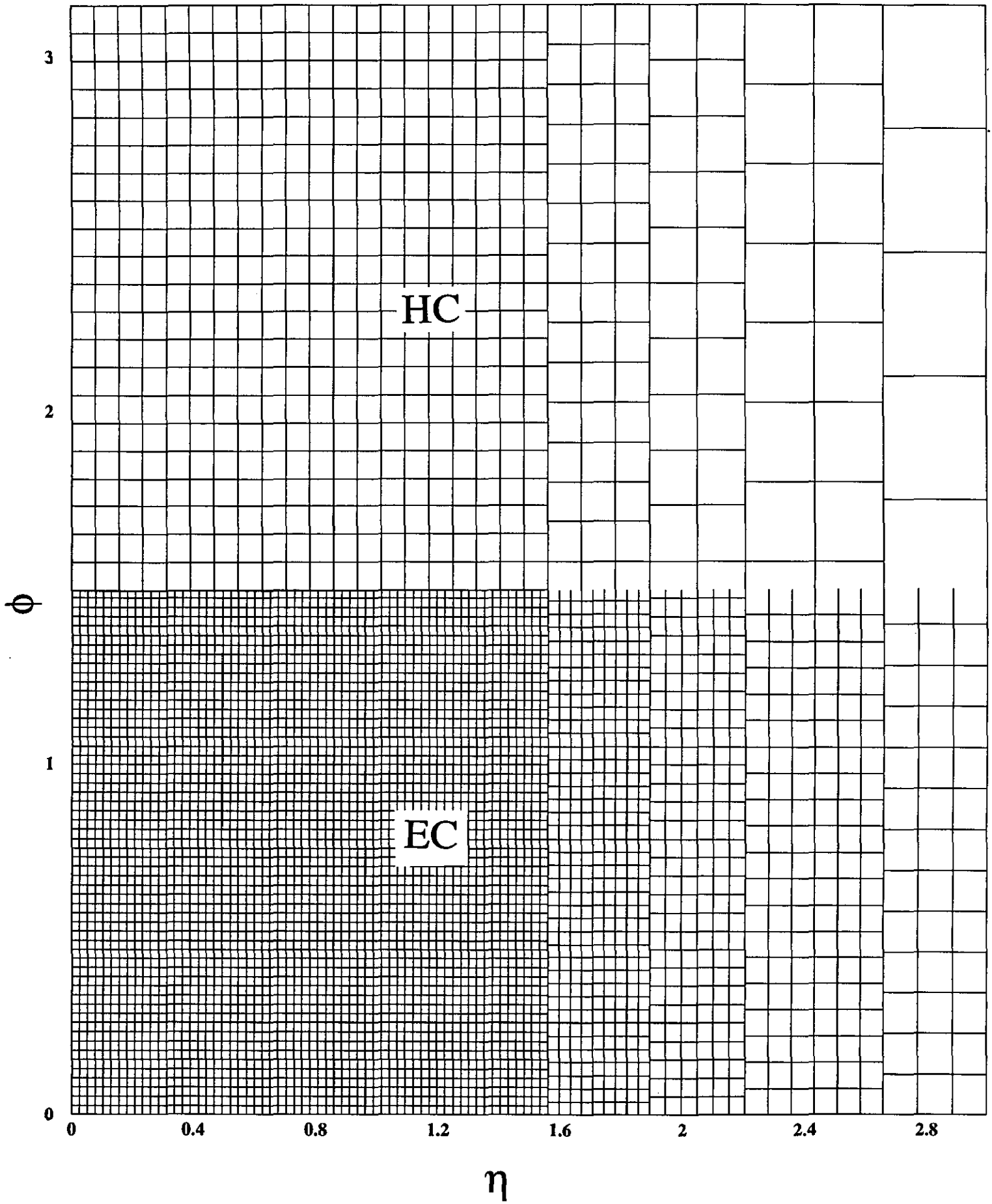

Figure 3: GEM calorimeter segmentation, as implemented in gemfast. (Figure provided by Henk Uijterwaal.)

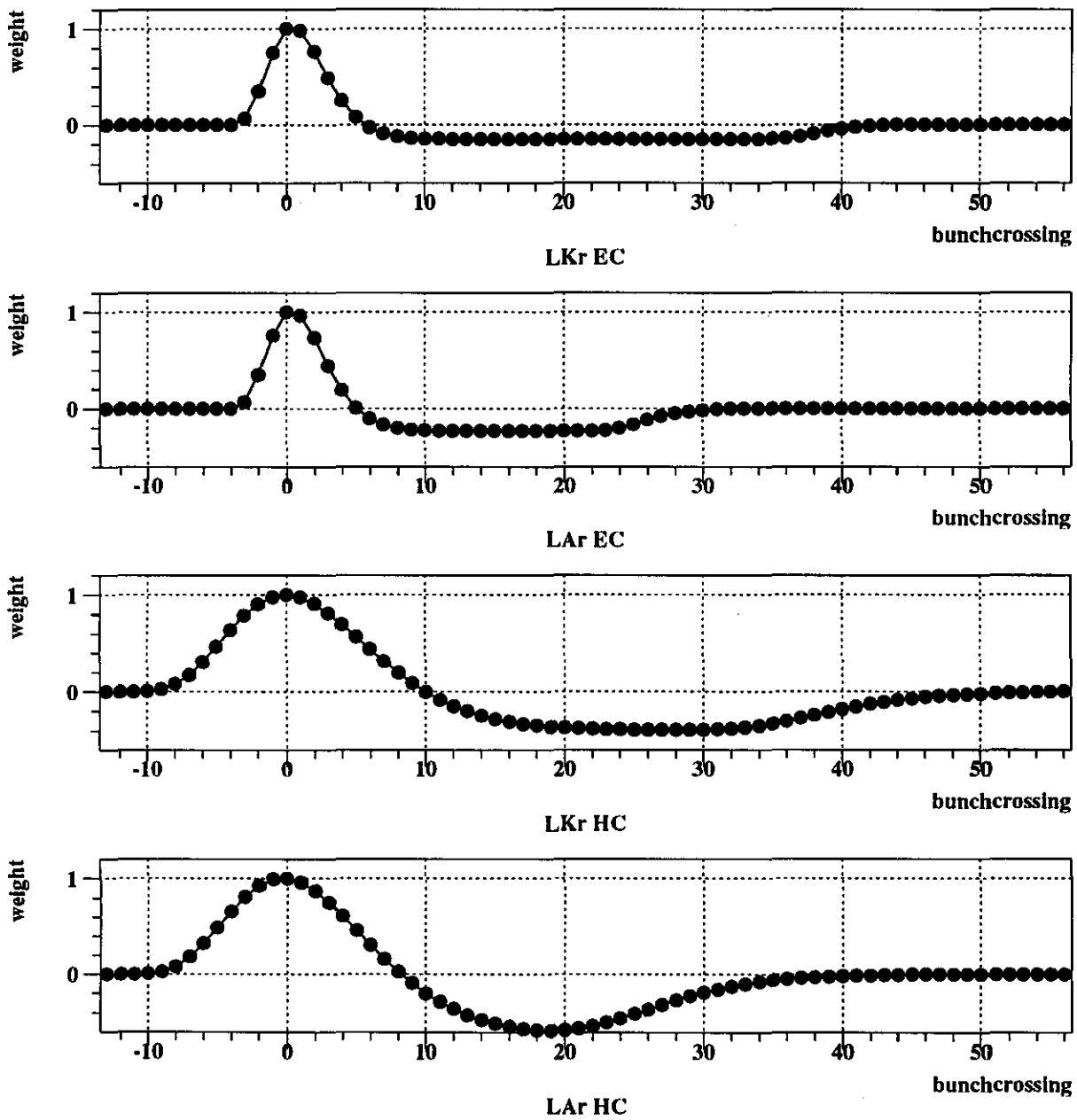

Figure 4: The signal waveforms, w_i vs the bunch crossing number, for different parts of the GEM calorimeter. The waveforms are normalized to 1 at the maximum.

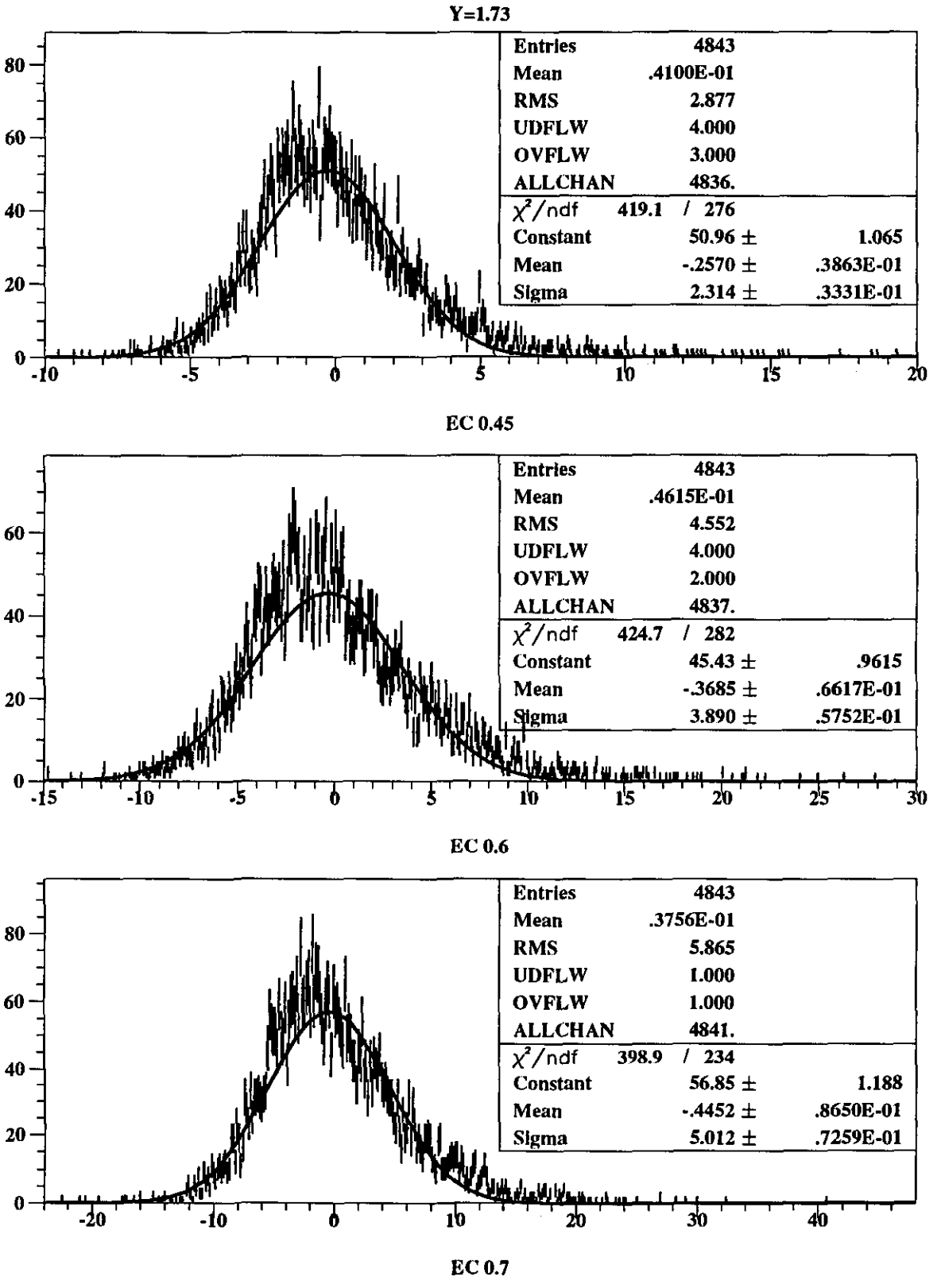

Figure 5: Pileup noise distributions in the EM endcap calorimeter for large cones.

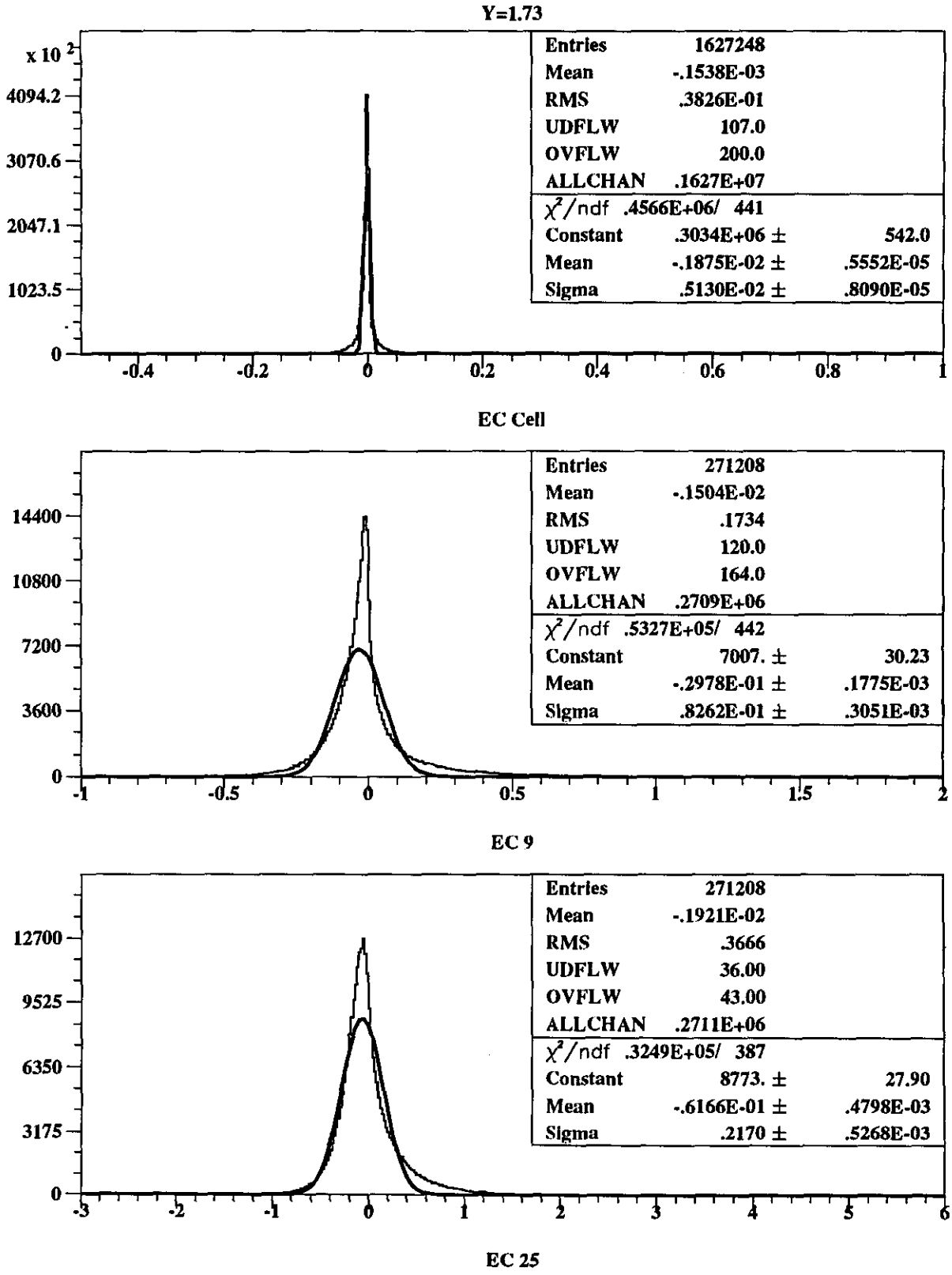

Figure 6: Pileup noise distributions in the EM endcap calorimeter for small areas. Pileup noise is non-gaussian because of the low pileup occupancy.

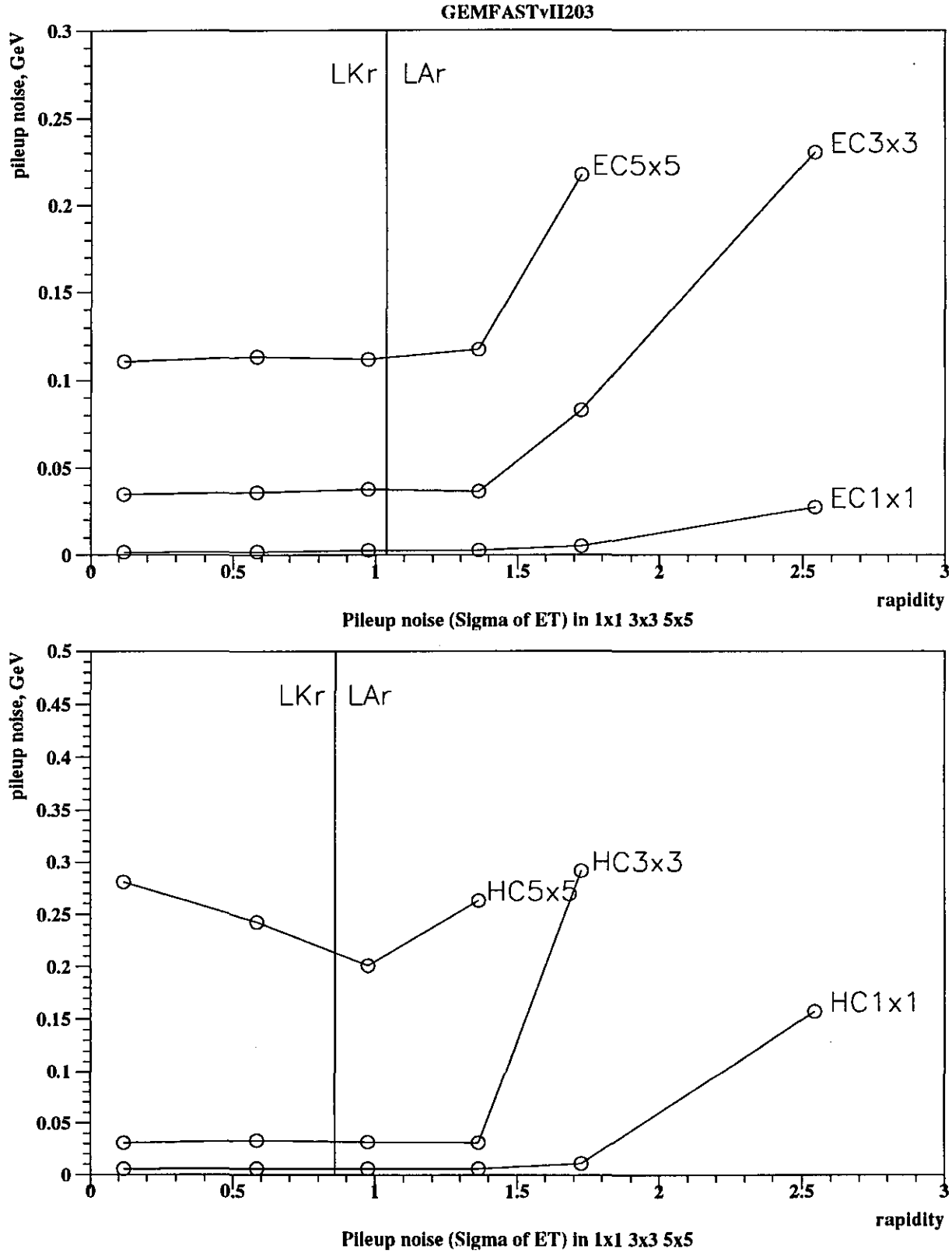

Figure 7: Pseudorapidity dependence of the pileup noise for 1 calorimeter cell, and for the 3×3 and 5×5 calorimeter towers. The top plot is for the EM section, the bottom plot is for the hadronic section. The increase of noise at large η is due to an increase of the size of the calorimeter towers in $\Delta\eta \times \Delta\phi$.

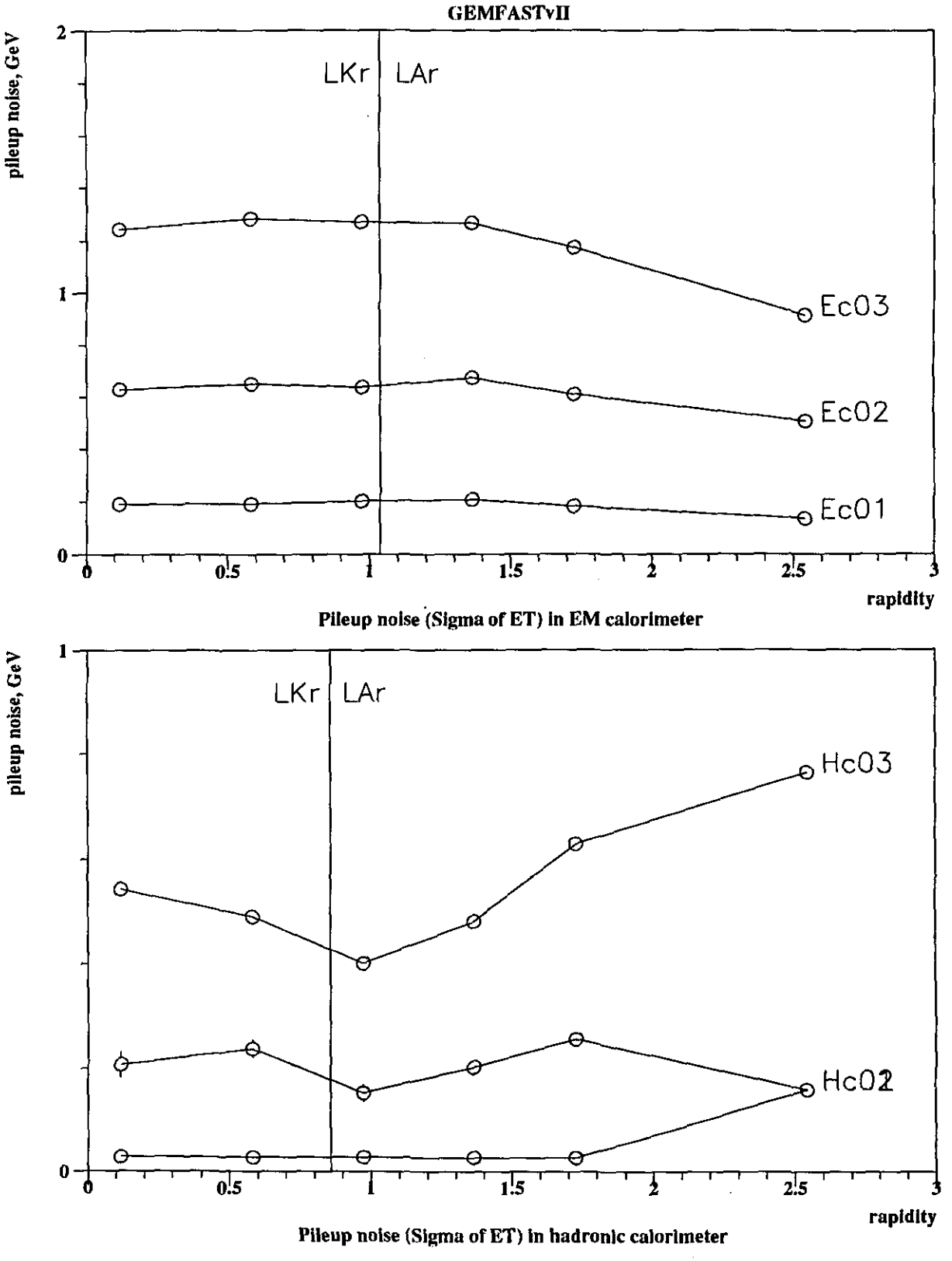

Figure 8: Pseudorapidity dependence of the pileup noise for a fixed small EM calorimeter area.

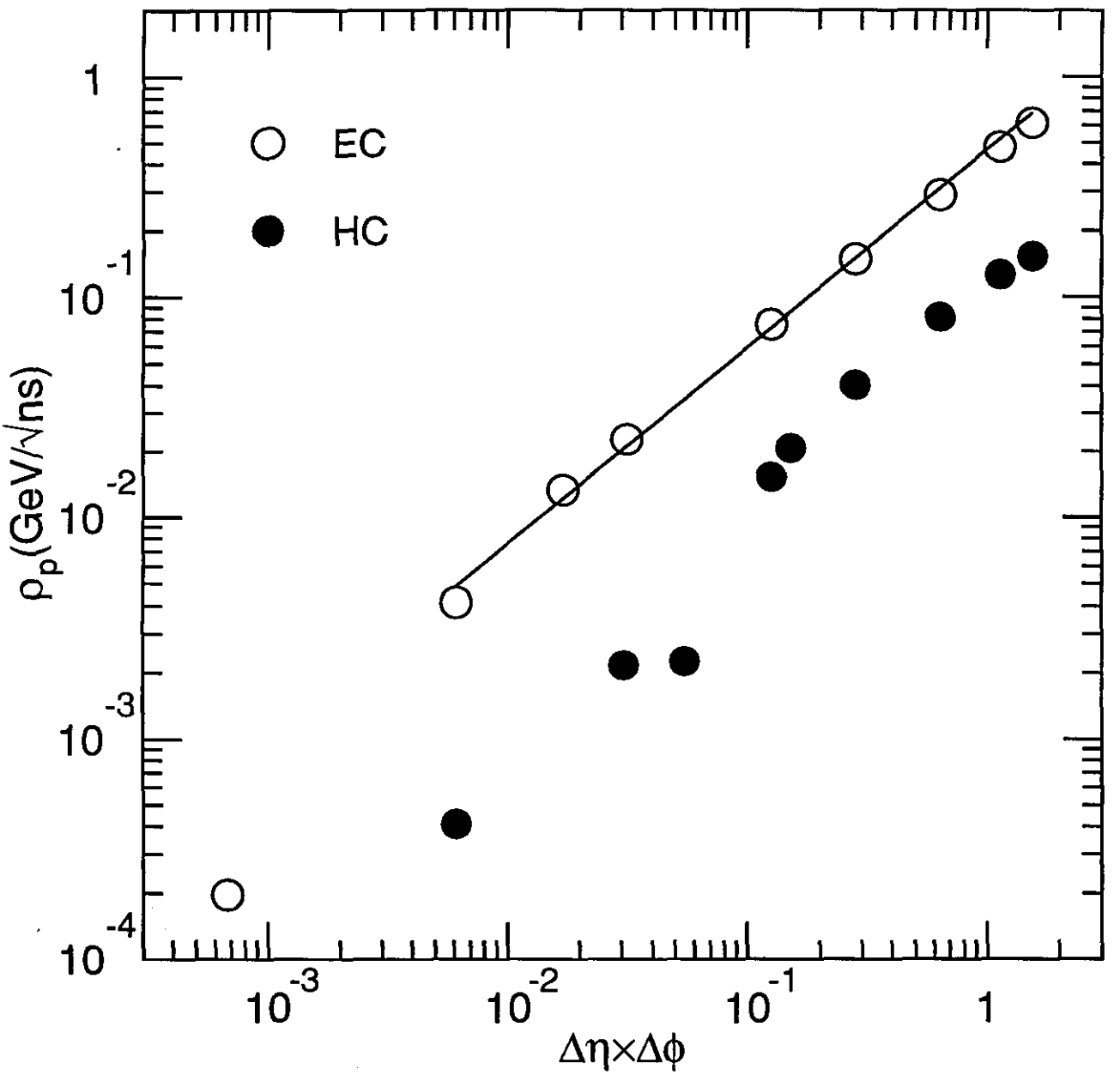

Figure 9: The dependence of the pileup noise on area for the EM (open circles) and hadronic (solid circles) calorimeter sections. The solid line represents the fit, described in the text.

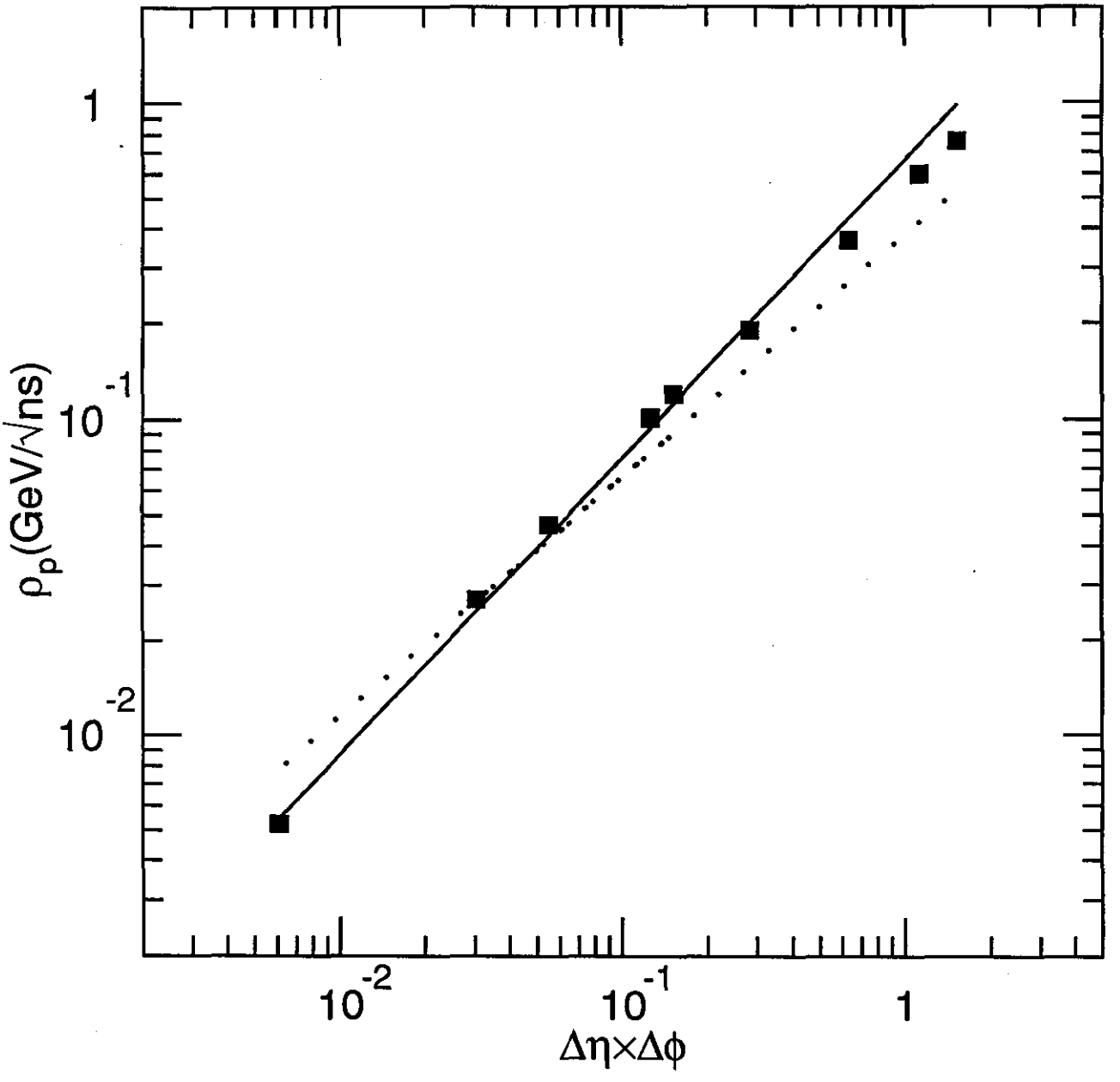

Figure 10: The dependence of the pileup noise on area for the sum of the EM and hadronic calorimeter sections at $\eta = 0.117$. The solid line is a fit to the data described in the text. Dotted line is the parameterization from [2]. The relatively small difference from the previous results [2] can be attributed to the use of a different event generator and shower parameterization algorithm.

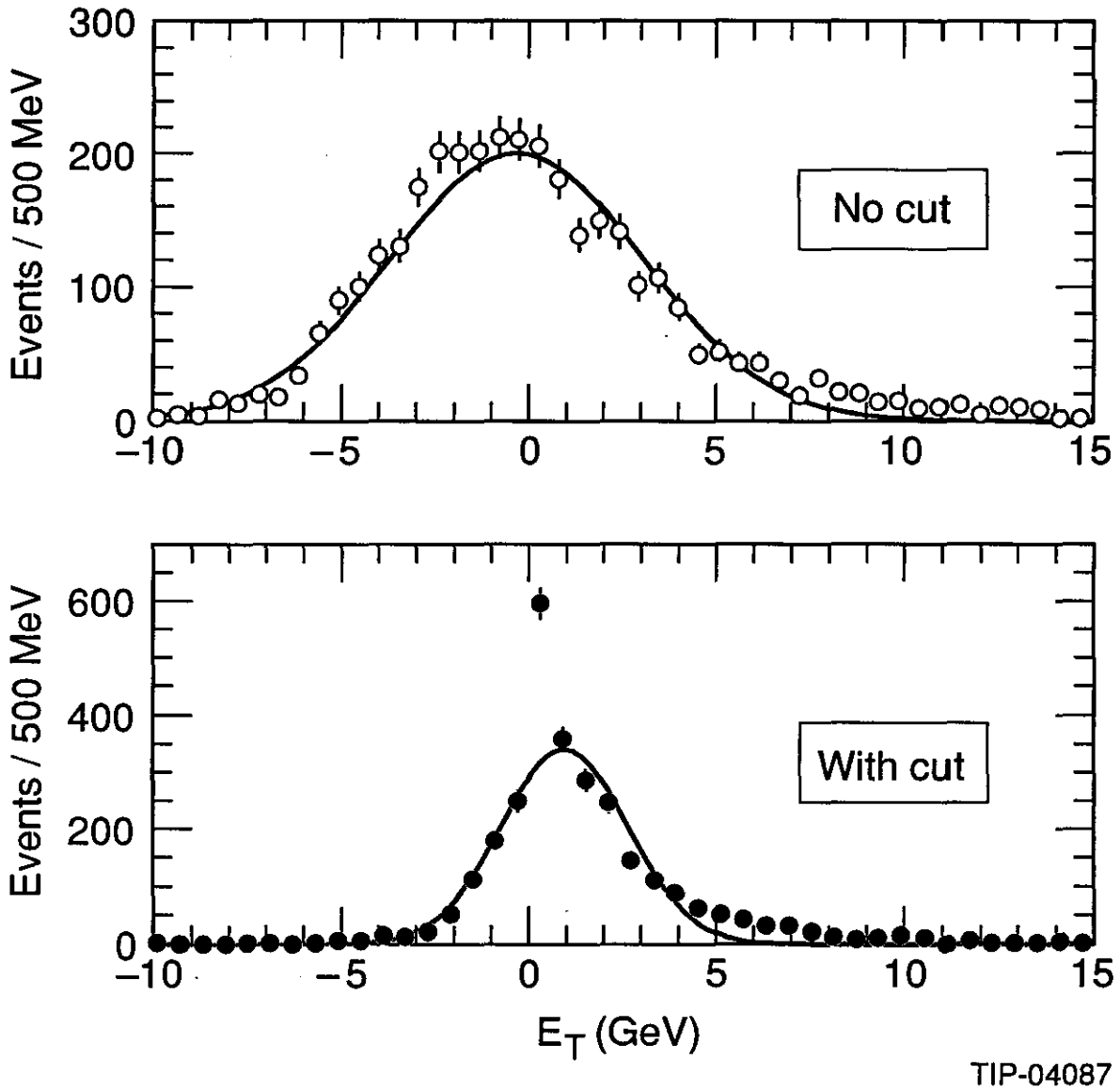

Figure 11: Distributions of the sum of thermal and pileup noise in a $R = 0.45$ cone, with Gaussian fits. The open and solid circles show the noise measured by summing all cells and by summing only cells with $|E_T| > 0.5$ GeV respectively.

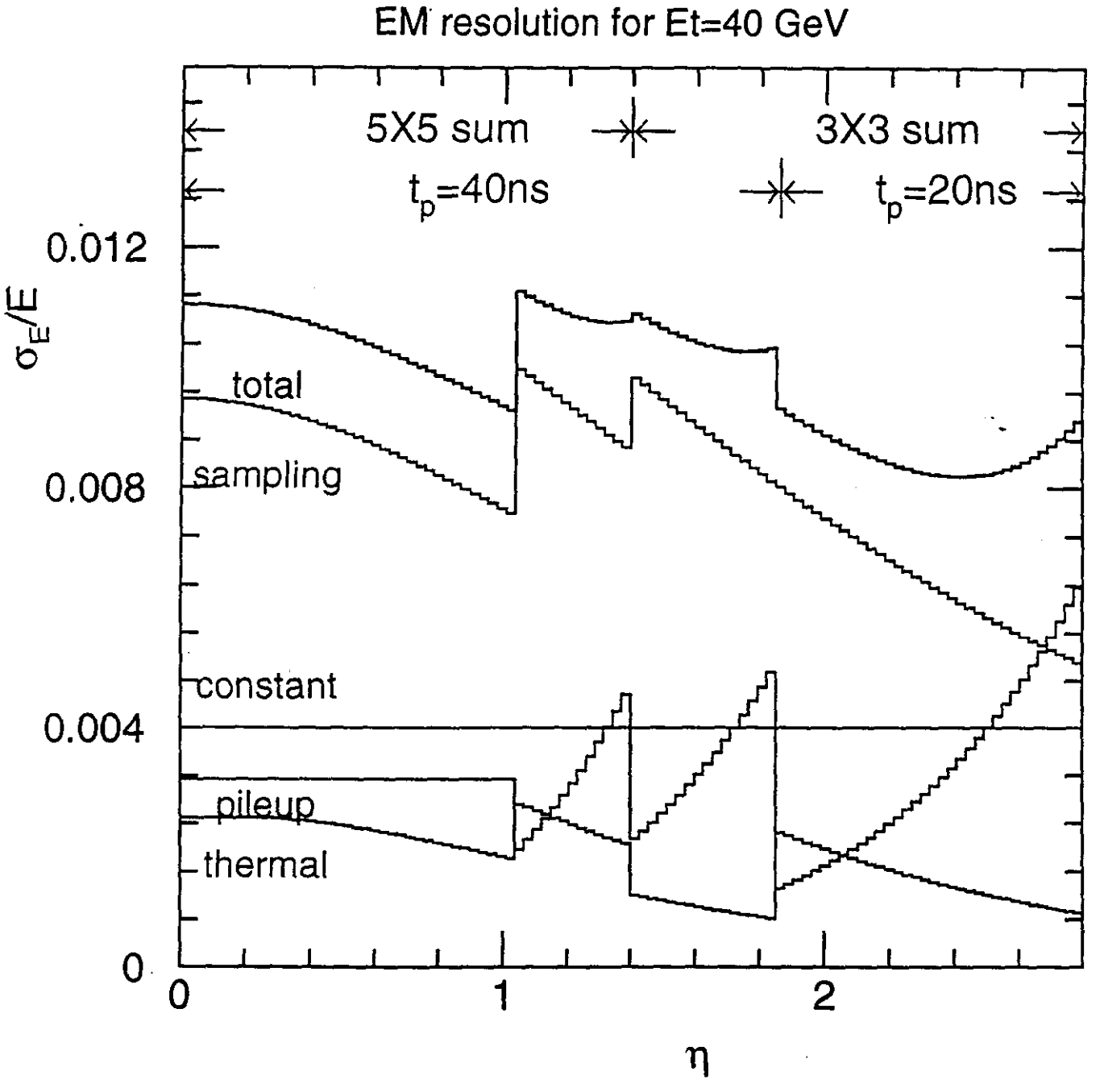

Figure 12: GEM EM calorimeter resolution, with the contribution of different factors. Figure provided by Hong Ma.